Brequinar and Dipyridamole in Combination Exhibits Synergistic Antiviral Activity Against SARS-CoV-2 *in vitro*: Rationale for a host-acting antiviral treatment strategy for COVID-19

Authors

James F. Demarest[a], Maryline Kienle[a], RuthMabel Boytz[b], Mary Ayres[c], Eun Jung Kim[d], Donghoon Chung[d], Varsha Gandhi[c], Robert Davey[b], David B. Sykes[a,e,f,g], Nadim Shohdy[a], John C. Pottage, Jr.[a], Vikram S. Kumar[a]*

[a] Clear Creek Bio, Cambridge, Massachusetts, USA

[b] NEIDL, Boston University, Boston, Massachusetts, USA

[c] Department of Experimental Therapeutics, MD Anderson Cancer Center, Houston, Texas, USA

[d] University of Louisville, Louisville, Kentucky, USA

[e] Center for Regenerative Medicine, Massachusetts General Hospital, Boston, MA.

[f] Harvard Stem Cell Institute, Cambridge, MA.

[g] Massachusetts General Hospital Cancer Center, Boston, MA.

*Corresponding author

KEYWORDS: Brequinar, dipyridamole, dihydroorotate dehydrogenase (DHODH), COVID-19, SARS-CoV-2

ABSTRACT

The continued evolution of severe acute respiratory syndrome coronavirus 2 (SARS-CoV-2) has compromised the efficacy of currently available vaccines and monoclonal antibody (mAb)-based treatment options for COVID-19. The limited number of authorized small-molecule direct-acting antivirals present challenges with pill burden, the necessity for intravenous administration or potential drug interactions. There remains an unmet medical need for effective and convenient treatment options for SARS-CoV-2 infection. SARS-CoV-2 is an RNA virus that depends on host intracellular ribonucleotide pools for its replication. Dihydroorotate dehydrogenase (DHODH) is a ubiquitous host enzyme that is required for de novo pyrimidine synthesis. The inhibition of DHODH leads to a depletion of intracellular pyrimidines, thereby impacting viral replication in vitro. Brequinar (BRQ) is an orally available, selective, and potent low nanomolar inhibitor of human DHODH that has been shown to exhibit broad spectrum inhibition of RNA virus replication. However, host cell nucleotide salvage pathways can maintain intracellular pyrimidine levels and compensate for BRQ-mediated DHODH inhibition. In this report, we show that the combination of BRQ and the salvage pathway inhibitor dipyridamole (DPY) exhibits strong synergistic antiviral activity in vitro against SARS-CoV-2 by enhanced depletion of the cellular pyrimidine nucleotide pool. The combination of BRQ and DPY showed antiviral activity against the prototype SARS-CoV-2 as well as the Beta (B.1.351) and Delta (B.1.617.2) variants. These data support the continued evaluation of the combination of BRQ and DPY as a broad-spectrum, host-acting antiviral strategy to treat SARS-CoV-2 and potentially other RNA virus infections.

39 ## INTRODUCTION

40 As of March 2022, there have been more than 6-million reported deaths and greater than 400-
41 million cases of coronavirus disease 2019 (COVID-19) worldwide as suggested by the World
42 Health Organization (WHO; https://covid19.who.int/). Furthermore, the number of infections
43 with severe acute respiratory syndrome coronavirus 2 (SARS-CoV-2), the causative agent of
44 COVID-19, likely exceeds the number of reported cases with an estimated excess mortality of
45 18.2 million [1]. Despite the availability of multiple prophylactic vaccines, SARS-CoV-2
46 continues to evolve, compromising the efficacy of vaccines and monoclonal antibody (mAb)-
47 based treatment options. Furthermore, there are only a handful of small-molecule antivirals
48 including two RNA-dependent RNA polymerase (RdRp) inhibitors, remdesivir and
49 molnupiravir, and one inhibitor of the SARS-CoV-2 main protease (Mpro), nirmatrelvir
50 (nirmatrelvir also requires the pharmacologic booster ritonavir in order to achieve sufficient
51 plasma drug levels). There remains therefore a high unmet medical need for safe, efficacious,
52 and patient-friendly treatments for SARS-CoV-2 infection.

53 While the therapeutic small molecules described above are direct-acting antivirals (DAAs) that
54 target virus-specific proteins, an alternative treatment strategy is to develop host-acting antivirals
55 (HAAs) that target host pathways essential for the viral lifecycle. A host-based mechanism of
56 action may provide unique advantages over DAAs including a greater likelihood of broad-
57 spectrum antiviral activity against several families of RNA viruses. In addition, HAAs may
58 possess an inherently higher barrier to the development of resistance when compared to DAAs as
59 host-targets typically remain unchanged in contrast to the rapid emergence of viral variants
60 containing mutations that decrease the efficacy of DAAs.

61 Dihydroorotate dehydrogenase (DHODH) is a host enzyme that is essential for *de novo*
62 pyrimidine synthesis and has emerged as a candidate target of HAAs. Brequinar (BRQ) is an
63 orally available, selective, and potent low nanomolar human DHODH inhibitor (DHODHI)
64 shown to deplete intracellular uridine, cytidine, and thymidine levels *in vitro* and *in vivo* [2, 3, 4].
65 As an antiviral approach, DHODHIs such as BRQ block the host production of cellular
66 pyrimidine nucleotide triphosphates (NTPs) required by viruses for replication [5, 6, 7, 8]. To
67 date, BRQ has been studied in multiple human clinical studies that have included more than 1000
68 subjects with viral infection, hematologic malignancies, or autoimmune disorders [Clear Creek
69 Bio data on file; 2, 3, 9, 10].

70 DHODHIs exhibit potent *in vitro* activity against several RNA viruses such as SARS-CoV-2,
71 influenza, Zika (ZKV), Dengue (DENV), respiratory syncytial virus (RSV), and Ebola (EBOV)
72 [5, 6, 7, 8]. Despite this promising *in vitro* data, the successful translation of DHODHI
73 monotherapy showing clinical benefit is lacking. While the DHODHI NITD-982 exhibited *in*
74 *vitro* antiviral activity against DENV, the *in vivo* treatment of infected mice had no effect on
75 viremia [11]. This is likely due to other pathways that can compensate for the reduction of
76 pyrimidine NTPs by DHODH inhibition such as the host nucleoside transporters (equilibrative
77 nucleoside transporters, ENT) that facilitate salvage via extracellular uridine and cytidine [12,
78 13]. The concentration of extracellular uridine in mammalian plasma may range up to 10 μM
79 [12] and may have contributed to limited clinical efficacy of DHODH inhibition in the oncology
80 setting [2].

81 A combination of DHODH and nucleotide salvage pathway inhibitors may therefore be required
82 for optimal therapeutic efficacy (**Figure 1**). Consistent with this hypothesis, the antiviral activity

83 of a DHODHI against DENV was enhanced by the addition of cyclopentenyl uracil, an inhibitor
84 of uridine salvage [14]. BRQ has also been shown to synergize with the ENT1/2/4 inhibitor
85 dipyridamole (DPY) which blocks the transport of extracellular pyrimidines needed for *in vitro*
86 growth of tumor cell lines [13]. DPY, FDA approved in 1961
87 [https://www.accessdata.fda.gov/drugsatfda_docs/label/2019/012836s061lbl.pdf], also inhibits
88 platelet aggregation and has widespread clinical use in combination with aspirin for the
89 secondary prevention of stroke
90 [https://www.accessdata.fda.gov/drugsatfda_docs/label/2012/020884s030lbl.pdf]. We chose to
91 evaluate the *in vitro* pharmacologic and antiviral activity of the combination of BRQ and DPY
92 (BRQ+DPY) in uninfected and SARS-CoV-2-infected A549/ACE2 cells.

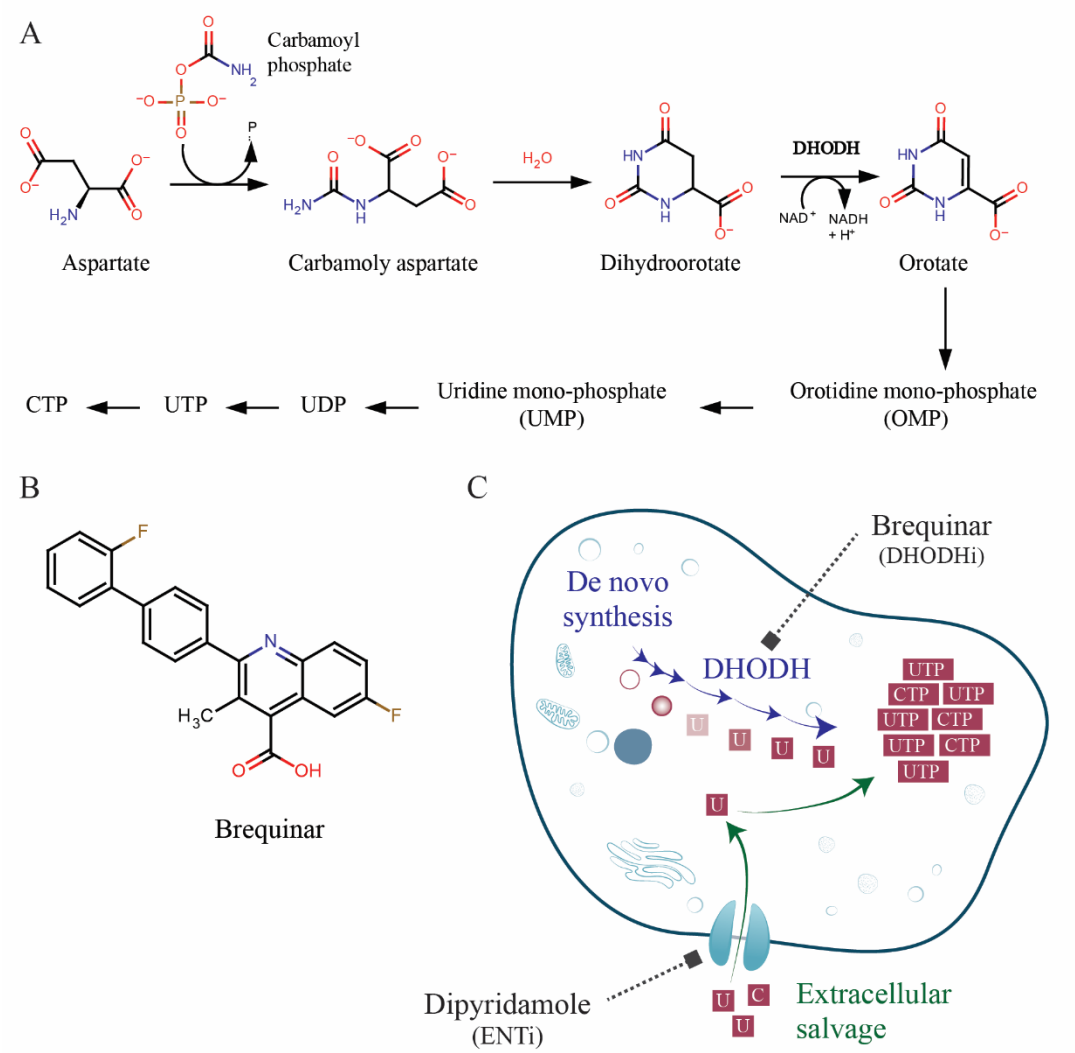

Figure 1: Rationale for combined DHODH and salvage pathway inhibition

RESULTS

DPY potentiates the suppression of pyrimidine NTPs by BRQ without apparent cytotoxicity

To study the effect of BRQ+DPY on the concentration of cellular pyrimidine nucleotides (CTP and UTP), uninfected A549/ACE2 cells were treated either with BRQ, DPY, or in combination, over an 8-hour time course. The A549/ACE2 cell line was derived from the parental lung

100 carcinoma A549 and engineered to express human ACE2, the entry receptor for SARS-CoV-2,
101 for use in antiviral assays. Cells were harvested after treatment at each time point (0, 1, 2, 4, and
102 8 hours) and the NTP concentrations were compared to the control group (T=0, DMSO treated)
103 (**Figure 2**).

104 The concentrations of purine nucleotides (ATP and GTP) were not decreased by any of the
105 treatments. As a single agent, DPY (1 μM) had no impact on either UTP or CTP levels relative
106 to control at time 0 (baseline). Single agent BRQ (1 μM) exhibited a reduction in pyrimidine
107 NTPs (CTP and UTP) concentrations starting at 4 h (16% and 33% decrease for CTP and UTP,
108 respectively) and the effect was more pronounced at 8 h (77.5% and 83.32% decrease for CTP
109 and UTP, respectively) (**Figure 2).** The combination of BRQ (1 μM) + DPY (1 μM)
110 demonstrated a potentiated effect compared to either agent alone. At 2 h, BRQ+DPY reduced
111 CTP and UTP from baseline by 33.6% and 47.3%, respectively. At 4 h, BRQ+DPY reduced CTP
112 and UTP concentrations from baseline by 71% and 79%, respectively; this was similar to what
113 was seen with BRQ alone at 8 h. At 8h, BRQ+DPY reduced CTP and UTP concentrations from
114 baseline by 86.6% and 91.6%, respectively. The effect of BRQ+DPY on pyrimidine NTP levels
115 was significant relative to DMSO controls and BRQ as a single agent (Supplementary Tables).

116 We queried whether the effect of BRQ+DPY on pyrimidine NTP concentrations was driven by
117 general cytotoxicity. The CC_{50} values for BRQ, DPY, or BRQ+DPY (1:1 ratio) were >10 μM
118 even after three days of exposure. Notably, these concentrations of BRQ and DPY are 10-fold
119 higher than those used to assay the inhibition of pyrimidine biosynthesis and nucleoside salvage,
120 respectively.

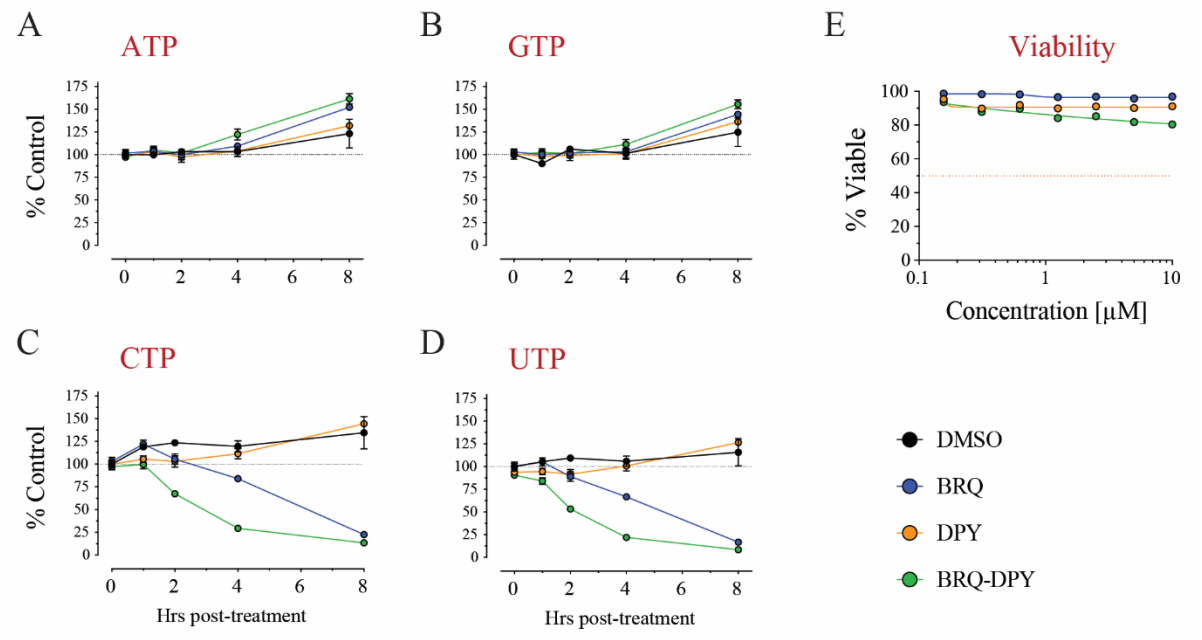

Figure 2. DPY potentiates the suppression of pyrimidine NTPs by BRQ without cytotoxicity. a-d) Changes in cellular nucleotide pools over 8 hours in response to the treatment of brequinar (BRQ; 1 μM) and dipyridamole (DPY; 1 μM) for single and combination treatment. Free NTP concentrations were normalized to the vehicle control group at 0 hours post treatment (n=3 per time point, per group). **e)** A549/ACE2 cell viability following treatment of BRQ and DPY for three days. Cell viability was measured with CellTiter-Glo and compared to the vehicle control group (DMSO treated).

BRQ+DPY suppresses pyrimidine nucleotides even with high exogenous uridine

Given the mechanism of action as a nucleoside transport inhibitor, we asked whether DPY could potentiate the BRQ-mediated decrease in concentration of pyrimidine NTPs even in the presence of higher concentrations of exogenous uridine. To address this, we repeated the experiment in the presence or absence of uridine (20 μM) at 4 h post compound addition in HEK-293T-hACE2 (**Figure 3A**) and A549/ACE2 cells (**Figure 3B**). Pyrimidine NTP levels were substantially

135 reduced with single agent BRQ (1uM) in both cell lines: HEK-293T-hACE2 (88% and 94%
136 decrease for CTP and UTP, respectively) and A549/ACE2 (56% and 63% decrease for CTP and
137 UTP, respectively). The combination of BRQ (1 μM) and DPY (1 μM) exhibited greater
138 reduction of pyrimidine NTP levels than BRQ alone in both HEK-293T-hACE2 (87% and 96%
139 decrease for CTP and UTP, respectively) and A549/ACE2 (91% and 94 % for CTP and UTP,
140 respectively) cells; the latter being consistent with our previous experiment (**Figure 2**).

141 The addition of excess uridine rescued cellular CTP and UTP concentrations in cells treated only
142 with BRQ. In contrast, and consistent with the pharmacological action of DPY, rescue of CTP
143 and UTP levels with excess uridine was not observed in cells treated with BRQ+DPY. Purine
144 NTP levels were not impacted by BRQ or DPY or the combination (data not shown). This result
145 confirms that blocking pyrimidine salvage potentiates the BRQ effect on intracellular pyrimidine
146 NTP concentrations in cells even in the presence of excess concentrations of extracellular
147 uridine.

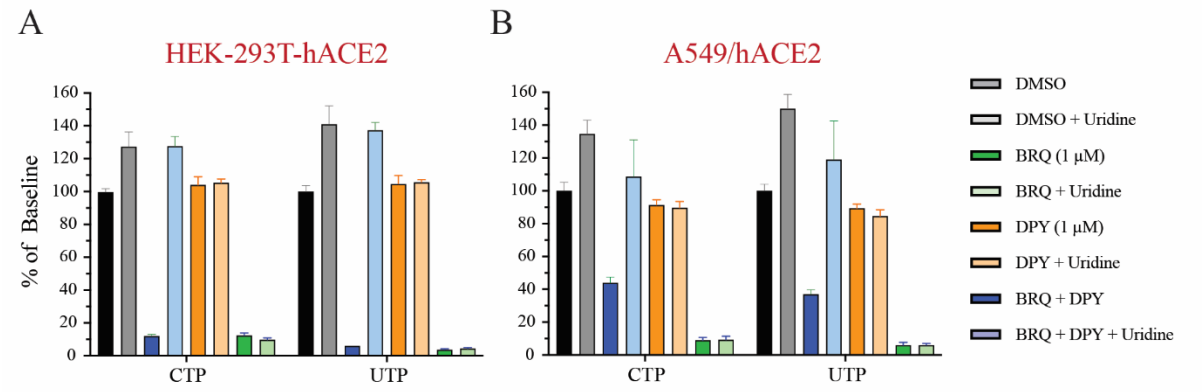

148

149 **Figure 3: BRQ+DPY suppresses levels of pyrimidine nucleotides even in presence of high**
150 **concentrations of exogenous uridine.** The ability of 1 μM BRQ or 1 μM DPY alone or in
151 combination to decrease intracellular pyrimidine nucleotides concentrations in HEK-293T-
152 hACE2 (Panel A) and A549/ACE2 (Panel B) at 4 h post compound addition; the effect of BRQ

153 alone was more pronounced in HEK-293T-hACE2 cells. The addition of excess exogenous
154 uridine (20 M) was able to rescue pyrimidine nucleotides inhibition by BRQ alone but not by the
155 combination BRQ+DPY in both HEK-293T-hACE2 and A549-ACE2 cells. Purine nucleotides
156 levels were unaffected in either cell type (data not shown).

157 BRQ+DPY exhibits synergistic antiviral activity *in vitro* against SARS-CoV-2

158 Given their mechanisms of action and our *in vitro* data showing that the combination of
159 BRQ+DPY rapidly lowers pyrimidine NTP pools which are required for viral RNA
160 synthesis/replication (**Figure 2**), we explored whether BRQ+DPY may also exhibit greater
161 antiviral activity than either agent alone.

162 *BRQ+DPY demonstrates synergistic antiviral activity*

163 The antiviral activity of BRQ+DPY inhibition was assessed in A549/ACE2 cells infected with
164 SARS-CoV-2 Beta variant (B.1.351) (**Figure 4**). DPY treatment alone had no impact on SARS-
165 CoV-2 infection (data not shown). The antiviral activity of BRQ was enhanced in a dose-
166 dependent manner by the addition of DPY (**Figure 4A** and **Table 1**). The decrease in EC_{50}
167 values was observed across pharmacologically relevant concentrations of DPY (0.78 μM or
168 1.563 μM; [15]); decreases from 2.67 μM for BRQ alone to 0.80 μM (3.3-fold lower) and to
169 0.59 μM (4.5-fold lower), respectively. Similar enhancement of BRQ antiviral activity with the
170 addition of DPY was also observed in separate experiments using Vero cells infected with
171 geographically distinct Wuhan-related SARS-CoV-2 strains (data not shown). The antiviral
172 activity of BRQ+DPY was not attributable to cellular cytotoxicity as cytotoxicity of BRQ and

173 DPY alone or as a combination of BRQ (5.0 μM max) and either DPY at 0.78 μM or 12.5 μM
174 was <50% in the MTT assay (Supplemental Figure S1).

175 To determine whether BRQ+DPY had additive, synergistic, or antagonistic interactions, the
176 antiviral data were analyzed using a combination of Loewe and Bliss models [16]. The 2-drug
177 combination of BRQ+DPY exhibited a strong synergistic interaction (**Figure 4B** and **Table 1**).
178 The average synergy score from three replicates was 22.6, with the most synergistic area
179 covering 75.2 arbitrary square units. These data confirm synergistic antiviral activity of
180 BRQ+DPY in the treatment of SARS-CoV-2 at pharmacologically relevant drug concentrations.

181 *Exogenous uridine supplementation partially abrogates the synergistic effect*

182 The effect of excess exogenous uridine on the antiviral activity of BRQ+DPY was more
183 pronounced at DPY concentrations <3 μM where substantial or complete reversal of antiviral
184 activity (e.g., EC_{50} > maximum concentration tested) was observed. DPY concentrations at or
185 above 6.25 μM decreased the impact of excess uridine (**Table 1, examples in Figure 4C**).
186 Consistent with the increase in EC_{50} values for BRQ+DPY in the presence of 20 μM uridine,
187 synergy analysis of infection data revealed a shift in synergistic dose combinations to higher
188 concentrations of both drugs (**Figure 4D**). Furthermore, the synergy score in the presence of
189 excess exogenous uridine was -4.7, which falls in the range of additivity. The additive score is in
190 part confounded by the apparent antagonism of excess uridine at low concentrations of DPY and
191 by the lesser effect at higher DPY concentrations. The physiological relevance of 20 μM uridine,
192 some 2- to 9-fold higher than physiologic levels [12], is not clear.

193 **Table 1. BRQ+DPY Synergy vs SARS-CoV-2 Beta (B.1.351)**

Treatment	EC_{50} [uM] No Added Uridine	Fold-Change vs BRQ Alone	EC_{50} [uM] With 20uM Uridine	Fold-Change vs BRQ Without Added Uridine
DPY Alone	>50	N/A	>50	N/A
BRQ Alone	2.67	1.00	>5	>1.87
BRQ + 0.195uM DPY	1.06	-2.51	>5	>4.70
BRQ + 0.390uM DPY	0.94	-2.85	>5	>5.34
BRQ + 0.789uM DPY	0.80	-3.35	>5	>6.27
BRQ + 1.563uM DPY	0.59	-4.50	1.09	1.84
BRQ + 3.125uM DPY	0.57	-4.66	0.90	1.57
BRQ + 6.250uM DPY	0.44	-6.12	0.63	1.44
BRQ + 12.5uM DPY	0.32	-8.24	0.40	1.23
BRQ + 25uM DPY	0.28	-9.48	0.28	1.00
BRQ + 50uM DPY	0.28	-9.53	0.27	1.00
Synergy				
Synergy Score (Ave)*	22.57	Synergy	-4.66	Additivity
Most Synergistic Area	75.15		58.36	

194 *Determined with ZIP (Bliss+Loewe); Synergy scores: >10.0 indicates synergy; -10 to 10

195 indicates additivity; < -10 indicates antagonism; N/A: Not Applicable.

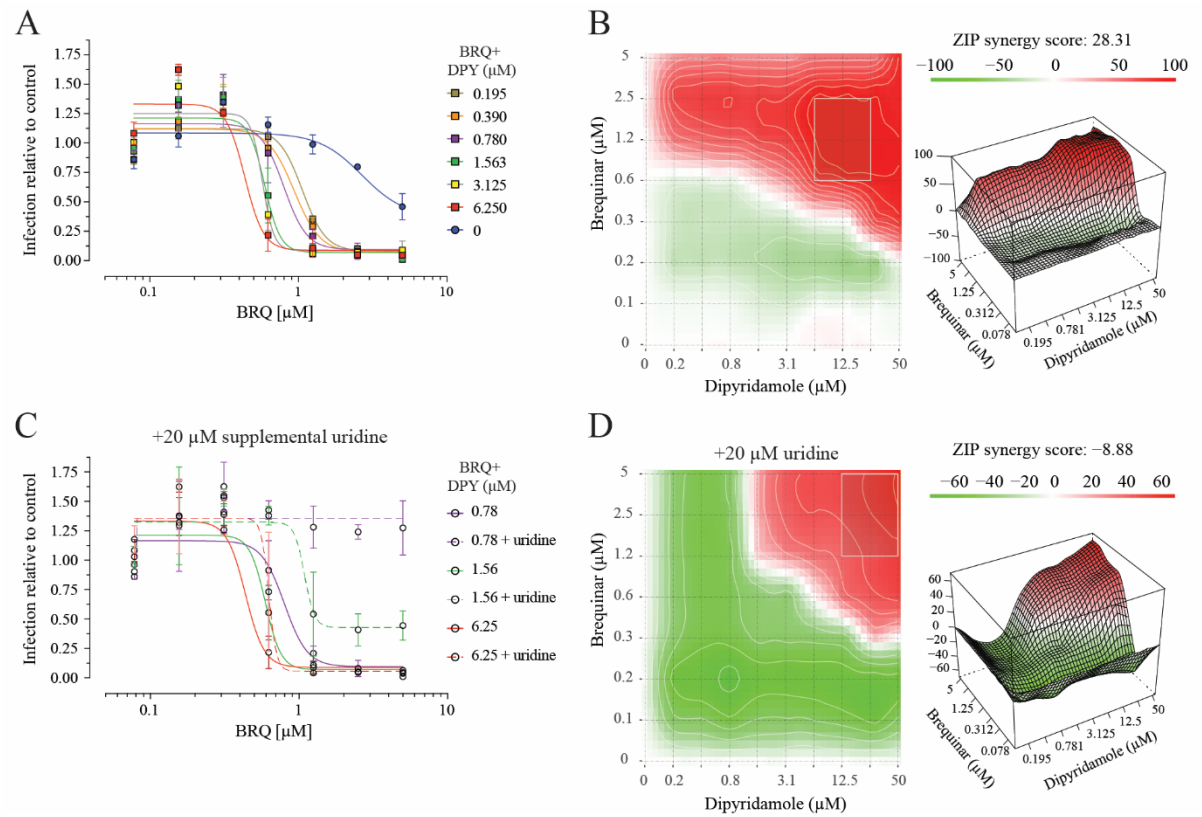

Figure 4: BRQ+DPY exhibits strong synergistic antiviral activity that is partially abrogated by supplementation of extracellular uridine. A) The antiviral activity of BRQ alone was enhanced in a dose-dependent manner by the addition of DPY. BRQ at concentrations of 0.078 – 5.0 μM alone or in combination with DPY at concentrations of 0.195 – 50.0 μM were evaluated. B) The 2-drug combination of BRQ+DPY exhibited strong synergy with highest effect observed at BRQ 0.6 – 2.5 μM and DPY 6.2 – 25 μM. C) The addition of excess exogenous uridine reduces the dose-dependent effect of BRQ+DPY. D) Addition of 20 μM uridine shifts the area of greatest synergy towards higher concentrations of both BRQ and DPY, and synergy scores suggest that uridine addition abrogates synergy still observed at higher DPY concentrations, rendering the effect of the drug combination overall as additive. A549-ACE2 cells were dosed with combinations of drugs and challenged with SARS-CoV-2 infection for 48 h. Infection was quantified from IFA images stained for SARS-CoV-2 N protein, and synergy

209 was calculated using SynergyFinder2.0 [16] under the LL4 curve and ZIP models. Dark red areas
210 and peaks in the contour plot indicate strong synergistic interaction, with the white box
211 representing the area of strongest synergy. Synergy scores greater than 10 indicate a synergistic
212 interaction, -10 to 10 suggests additivity, and less than -10 supports antagonism.

213 *BRQ antiviral activity against SARS-CoV-2 Delta Variant of Concern (B.1.617.2) is enhanced*
214 *with low concentrations of DPY*

215 Based on the findings with SARS-CoV-2 Beta (B.1.351), the antiviral activity of BRQ+DPY
216 was evaluated in the same assay system using the SARS-CoV-2 Delta variant of concern (VOC)
217 (B.1.617.2) (**Figure 5**). BRQ+DPY also exhibited enhanced antiviral activity against SARS-
218 CoV-2 Delta (B.1.617.2), relative to DMSO control as well as single agent BRQ.

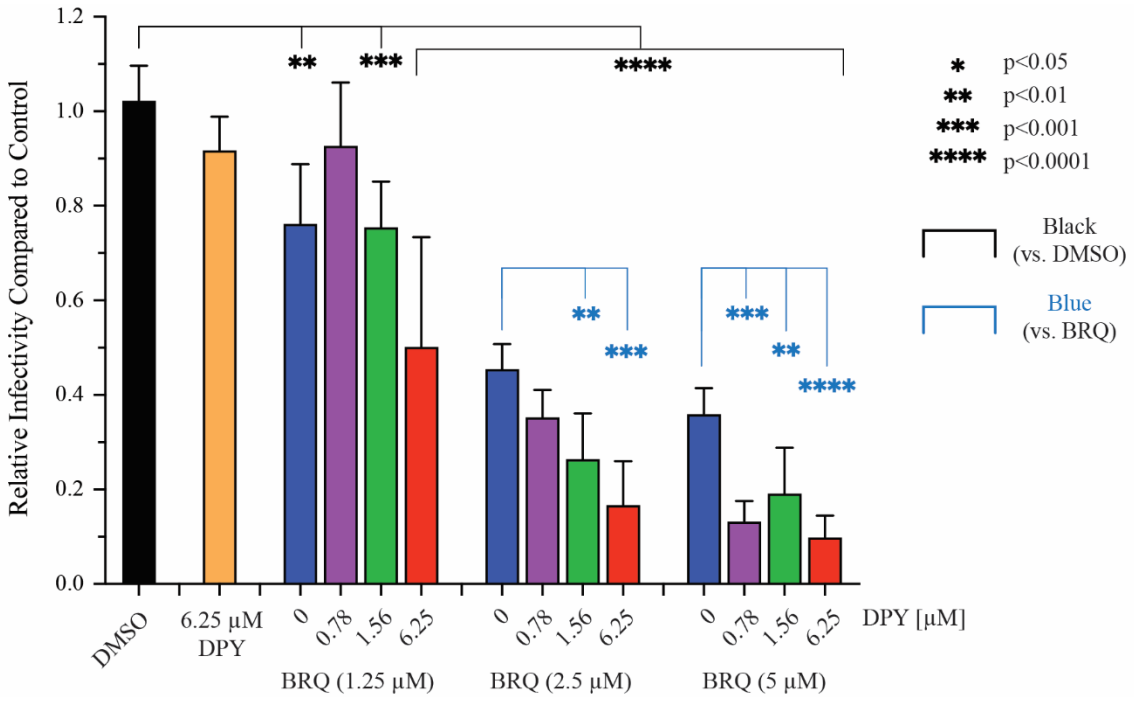

219

220 **Figure 5: BRQ antiviral activity against SARS-CoV-2 Delta VOC (B.1.617.2) is enhanced**
221 **with low concentrations of DPY.** The antiviral activity of BRQ alone was enhanced in a dose-

222 dependent manner by the addition of low concentrations of DPY. BRQ at concentrations of 1.25,
223 2.5 and 5.0

224 alone or in combination with DPY at concentrations of 0.78, 1.56, and 12.5 μM were evaluated.
225 A549-ACE2 cells were dosed with combinations of drugs and challenged with SARS-CoV-2
226 infection for 48 h. Infection was quantified from IFA images stained for SARS-CoV-2 N protein.

227 ## DISCUSSION

228 There remains a significant unmet medical need for safe and convenient treatments for people
229 infected with SARS-CoV-2. The most recently authorized antivirals have challenges with pill
230 burden, inconvenient routes of administration, or potential drug interactions. The potential
231 efficacy of DHODHI monotherapy for treatment of viral infection in humans remains to be
232 proven. Clinical experience in the oncology space suggests that the impact of available
233 extracellular uridine and the activity of nucleoside transporters may limit the efficacy of
234 DHODHI monotherapy. The *in vitro* antiviral activity of BRQ alone against SARS-CoV-2 has
235 been reported by others [17, 18, 19]. Given the growing evidence suggesting that DHODH
236 inhibition alone *in vitro* may not translate to *in vivo* activity, we explored a host-target antiviral
237 strategy with the combination BRQ and DPY.

238 The addition of DPY enhanced the inhibitory effect of BRQ on the concentration of intracellular
239 pyrimidine NTPs *in vitro*. This effect was consistent in the HEK-293T-hACE2 and A549/ACE2
240 cell lines (**Figs 2-3**) as well as multiple other cell lines and primary cells (data not shown). The
241 depletion of pyrimidine NTP pools by BRQ could be overcome with the addition of excess
242 exogenous uridine (20 μM) whereas the inhibitory activity of BRQ+DPY was preserved in the

243 setting of high concentrations of extracellular uridine. Furthermore, the inhibitory activity
244 associated with low concentrations of BRQ and DPY was not driven by apparent cytotoxicity.

245 Within a cell infected with SARS-CoV-2, more than 50% of RNA transcripts are viral RNA
246 transcripts, and all nucleotides are host-derived [20]. Thus, potent reduction of pyrimidine NTP
247 pools by the combination of BRQ+DPY should effectively limit viral replication. In A549/ACE2
248 cells (**Figure 4**), DPY alone had no evidence of antiviral effect against SARS-CoV-2 Beta
249 (B.1.351) and BRQ had marginal single agent activity consistent with published reports [17, 18,
250 19] and Clear Creek Bio data (not shown). Consistent with the enhanced *in vitro* reduction of
251 pyrimidine NTP levels in uninfected cells with 1 μM BRQ (**Figure 2**), the addition of DPY
252 increased the antiviral activity of BRQ alone in a dose-dependent manner (**Figure 4A** and **Table**
253 **1**). It is worth noting that as with the *in vitro* analyses of pyrimidine NTP levels, the antiviral
254 activity of BRQ+DPY was evident at concentrations with potential pharmacologic relevance,
255 <2 μM each [Clear Creek Bio data on file; 9, 15] and was not driven by apparent cytotoxicity
256 even at high concentrations. The analysis of 2-drug antagonism or additivity/synergy using a
257 combination of Loewe and Bliss models demonstrated strong synergy for the combination of
258 BRQ+DPY.

259 The addition of excess exogenous uridine abrogated the antiviral activity of BRQ in combination
260 with lower concentrations of DPY in SARS-CoV-2 infected A549/ACE2 cells though this
261 abrogation was less pronounced at the higher DPY concentrations (**Figure 4C and Table 1**). The
262 synergy analysis in the presence of 20 μM uridine shifted from synergy to additivity. These data
263 highlight the importance of extracellular uridine in maintaining cellular pyrimidine NTP levels

264 and supports the concept that inhibiting both *de novo* and salvage pyrimidine pathways with
265 BRQ+DPY merits further exploration.

266 A major area of concern is the development of viral resistance, as seen with selective pressures
267 by DAAs, or viral escape from immune pressures that lead to the emergence of novel SARS-
268 CoV-2 VOCs, as has been observed after vaccination and the development of natural immunity.
269 As BRQ and DPY target host rather than viral proteins, the antiviral activity of BRQ+DPY
270 should have limited liability with respect to viral escape or development of resistance. Our data
271 demonstrated comparable antiviral activity of BRQ+DPY against SARS-CoV-2 strains including
272 those like the original Wuhan-1 as well as Beta and Delta variants of concern.

273 Given the *in vitro* synergy against multiple SARS-CoV-2 strains in different cell types, a similar
274 enhancement of BRQ antiviral activity may be observed *in vivo* with the host-based combination
275 treatment of BRQ+DPY. Furthermore, given this synergy and the inability of excess exogenous
276 uridine to reverse this, the HAA combination of BRQ + DPY may be expected to present a high
277 barrier to the development of clinically relevant resistance relative to DAAs. This needs to be
278 formally assessed in clinical trials.

279 In this report, we demonstrated that the combination of BRQ+DPY significantly reduces
280 pyrimidine NTP levels which translates to synergistic antiviral activity against SARS-CoV-2
281 variants *in vitro*. The antiviral activity observed with BRQ+DPY at pharmacologically relevant
282 concentrations supports continued investigation of this combination as an oral treatment
283 approach for COVID-19. A small, outpatient Phase 2 clinical trial is currently underway to
284 evaluate this concept. [https://clinicaltrials.gov/ct2/show/NCT05166876]. Finally, if this

285 approach is successful, investigation of the use of BRQ+DPY in other RNA viral infections may
286 be warranted.

287 MATERIALS AND METHODS

288 Test Articles

289 Brequinar (Selleck Chemicals, Cat# S6626) and dipyridamole (Sigma Aldrich Prod# D9766)
290 were provided by Clear Creek Bio. Uridine was obtained from Sigma (Cat#: U3003-5G) and
291 Alfa Aesar/Fisher (AAA1522706) for the NTP and antiviral assays, respectively.

292 Cell lines and virus

293 A549/ACE2 and HEK-293T-hACE2 (BEI resources, NR-53821 and NR-52511) cells were
294 cultured in DMEM media supplemented with 10% FBS and 2 mM L-glutamine. Cells were
295 passed twice in a week and maintained at 37° C with 5 % CO_2. The absence of mycoplasma
296 contamination was validated regularly with a PCR-based method (ATCC, Universal
297 Mycoplasma Detection Kit, 30-1012K).

298 *In vitro* determination of BRQ+DPY effect on pyrimidine NTPs

299 Cells were plated in 6-well plates (200,000 cells/well) one day prior to experiment. Test
300 compounds were dissolved in DMSO as a stock and then diluted in culture media before testing.
301 The final concentration of DMSO was kept at 0.25%. For drug treatment, cell supernatant was
302 removed and replaced with media containing test compounds (n=3 per group). At timepoints
303 denoted, cell lysates were prepared according to a protocol published [21] with minor
304 modifications. In brief, cells were washed with PBS and treated with 0.75 mL of with 0.4 N

305 perchloric acid (PCA) on ice and harvested. Extracts were centrifuged (1500 rpm) and
306 supernatants were combined with a second 0.25 ml extraction. Extracts were combined and
307 neutralized with 10 N and 1 N KOH. Neutralization was determined using pH paper. Samples
308 were stored at -20°C until. The NTP concentrations of samples were analyzed with HPLC.

309 PCA extracts were analyzed using either a Waters 2695e HPLC with a Waters 2489 UV/Visible
310 detector or a Waters 2695 HPLC with a Waters 2487 Dual λ Absorbance detector. A Partisil 10
311 SAX column separated nucleoside triphosphates at a flow rate of 1.5 ml/min with a 50-minute
312 concave gradient curve (curve 8) from 60% 0.005 M NH4H2PO4 (pH 2.8) and 40% 0.75 M
313 NH4H2PO4 (pH 3.8) to 100% 0.75 M NH4H2PO4 (pH 3.8). Standard ribonucleotides were used
314 to create a standard curve, which was used to quantitate nucleotide pools [21].

315 Analysis of Variance with Dunnett's Multiple Comparisons Test was used to test for significant
316 differences from the DMSO Control at Time 0 vs all other conditions or DMSO vs BRQ, DPY,
317 or BRQ+DPY treatment at each timepoint (Supplemental Tables S1 and S2).

318 For assessment of potential cytotoxicity, cells were seeded in 96-well white plates at a density of
319 12,000 cells per well and cultured overnight. The next day, test compound diluted in cell culture
320 media were added to the cells at the final concentration from 50 μM to 0.4 μM, 8 points by 2-
321 fold serial dilution. After three days of incubation, cell viability was evaluated with CellTiter-
322 Glo, measuring luminescence with Synergy 4 (Biotek). 1% of Triton-X100 and 0.25% DMSO
323 were used as the positive and negative control, 0 and 100% cell viability, respectively.

324 BRQ+DPY antiviral experiments

325 A549/ACE2 cells were plated in 96-well plates at a density of 10,000 cells per well in RPMI
326 supplemented with 10% FBS and allowed to adhere overnight. The following day cells were
327 treated with 2-fold dilution series in triplicate of brequinar (ranging 5 μM – 0.0781 μM) and
328 dipyridamole (ranging 50 μM – 0.195 μM) in a matrix format allowing each concentration pair
329 to be tested. Dilution series of each compound alone were included on each plate, as well as
330 10 μM remdesivir positive control and DMSO negative control wells. Exogenous uridine
331 (20 μM) was added to an additional three plates to test whether brequinar inhibition of DHODH-
332 catalyzed uridine synthesis can be overcome by addition of excess uridine. Following one hour
333 of incubation with compounds, cells were challenged with approximately 400 FFU of SARS-
334 CoV-2 Beta (B.1.351; hCoV-19/USA/MD-HP01542/2021) and incubated at 37 ºC for 48 h. In a
335 separate experiment using A549/ACE2 cells, dilution series of brequinar and dipyridamole alone
336 or brequinar + 0.78 μM or 12.5 μM dipyridamole were tested with the SARS-CoV-2 Delta VOC
337 (B.1.617.2). Pre-treatment time, infection dose, and length of infection were the same as with
338 Beta variant. Analysis of Variance with Dunnett's Multiple Comparisons Test was used to test
339 for significant differences from the DMSO Control vs BRQ or BRQ+DPY treatment or between
340 BRQ alone vs BRQ+DPY.

341 Immunofluorescence detection of SARS-CoV-2 infection efficiency

342 Following 48 h of infection plates were fixed in 10% formalin for at least 6 h before removal
343 from the high containment laboratory. Plates were washed in PBS, permeabilized in 0.1% Triton
344 X-100 for 15 min at room temperature and blocked in 3.5% BSA for at least 1 h at room
345 temperature. To detect infection, plates were incubated overnight at 4 ºC with a rabbit anti-N

346 protein monoclonal antibody (SioBiological 40143-R004) diluted 1:20,000. Plates were washed
347 and treated with an AF488-conjugated goat anti-rabbit secondary antibody for 2 h at room
348 temperature. Finally, Hoechst33342 was added to visualize cell nuclei. Plates were imaged on a
349 Cytation 1 Multimode Plate Reader (BioTek) using a 4X objective lens. Infection efficiency,
350 defined as GFP-positive cells divided by total nuclei, was calculated for each image using a
351 CellProfiler pipeline.

352 ## Synergy calculations

353 Drug synergy was calculated with SynergyFinder2.0 [16] using inhibition readout, LL4 curve
354 fitting, and ZIP model parameters.

355 ## ACKNOWLEDGEMENTS

356 We thank Cindy Motaka for assistance in editing, Dr Olga Kharchenko for assistance with
357 Figure 1, Dr Justin Patten (Davey Lab) for help with antiviral assay development and Dr. David
358 Hesson for assistance in experimental design. J.F.D, M.K, J.C.P. Jr, N.S., D.B.S., and V.S.K.
359 hold equity in Clear Creek Bio. M.K. and V.S.K are employees of Clear Creek Bio. V.G., D.C.,
360 J.F.D, N.S, J.C.P. Jr, and D.B.S. are paid consultants of Clear Creek Bio. D.B.S. holds equity in
361 SAFI Biosolutions. Clear Creek Bio funded all work described in this article, including
362 Sponsored Research Agreements with Boston University, MD Anderson Cancer Center and the
363 University of Louisville.

364 REFERENCES

365 1. COVID-19 Excess Mortality Collaborators. 2022. Articles Estimating excess mortality due to
366 the COVID-19 pandemic: a systematic analysis of COVID-19-related mortality, 2020–21.
367 The Lancet https://doi.org/https://doi.org/10.1016/ S0140-6736(21)02796-3.
368 2. Peters GJ, Schwartsmann G, Nadal JC, Laurensse EJ, Groeningen CJ van, Vijgh WJ van der,
369 Pinedo HM. 1990. In vivo inhibition of the pyrimidine de novo enzyme dihydroorotic acid
370 dehydrogenase by brequinar sodium (DUP-785; NSC 368390) in mice and patients. Cancer
371 Res 50:4644–9.
372 3. Peters G, Kraal I, Pinedo H. 1992. In vitro and in vivo studies on the combination of
373 Brequinar sodium (DUP-785; NSC 368390) with 5-fluorouracil; effects of uridine. Brit J
374 Cancer 65:229–233.
375 4. Sykes DB, Kfoury YS, Mercier FE, Wawer MJ, Law JM, Haynes MK, Lewis TA,
376 Schajnovitz A, Jain E, Lee D, Meyer H, Pierce KA, Tolliday NJ, Waller A, Ferrara SJ,
377 Eheim AL, Stoeckigt D, Maxcy KL, Cobert JM, Bachand J, Szekely BA, Mukherjee S, Sklar
378 LA, Kotz JD, Clish CB, Sadreyev RI, Clemons PA, Janzer A, Schreiber SL, Scadden DT.
379 2016. Inhibition of Dihydroorotate Dehydrogenase Overcomes Differentiation Blockade in
380 Acute Myeloid Leukemia. Cell 167:171-186.e15.
381 5. Qing M, Zou G, Wang Q-Y, Xu HY, Dong H, Yuan Z, Shi P-Y. 2010. Characterization of
382 Dengue Virus Resistance to Brequinar in Cell Culture. Antimicrob Agents Ch 54:3686–3695.
383 6. Adcock RS, Chu Y-K, Golden JE, Chung D-H. 2017. Evaluation of anti-Zika virus activities
384 of broad-spectrum antivirals and NIH clinical collection compounds using a cell-based, high-
385 throughput screen assay. Antivir Res 138:47–56.

386 7. Bonavia A, Franti M, Keaney EP, Kuhen K, Seepersaud M, Radetich B, Shao J, Honda A,
387 Dewhurst J, Balabanis K, Monroe J, Wolff K, Osborne C, Lanieri L, Hoffmaster K, Amin J,
388 Markovits J, Broome M, Skuba E, Cornella-Taracido I, Joberty G, Bouwmeester T, Hamann
389 L, Tallarico JA, Tommasi R, Compton T, Bushell SM. 2011. Identification of broad-
390 spectrum antiviral compounds and assessment of the druggability of their target for efficacy
391 against respiratory syncytial virus (RSV). Proc National Acad Sci 108:6739–6744.
392 8. Park J-G, Ávila-Pérez G, Nogales A, Blanco-Lobo P, Torre JC de la, Martínez-Sobrido L.
393 2020. Identification and Characterization of Novel Compounds with Broad-Spectrum
394 Antiviral Activity against Influenza A and B Viruses. J Virol 94.
395 9. Joshi AS, King SP, Zajac BA, Makowka L, Sher LS, Kahan BD, Menkis AH, Stiller CR,
396 Schaefle B, Kornhauser DM. 1997. Phase I Safety and Pharmacokinetic Studies of Brequinar
397 Sodium after Single Ascending Oral Doses in Stable Renal, Hepatic, and Cardiac Allograft
398 Recipients. J Clin Pharmacol 37:1121–1128.
399 10. Madak JT, Bankhead A, Cuthbertson CR, Showalter HD, Neamati N. 2019. Revisiting the
400 role of dihydroorotate dehydrogenase as a therapeutic target for cancer. Pharmacol Therapeut
401 195:111–131.
402 11. Wang Q-Y, Bushell S, Qing M, Xu HY, Bonavia A, Nunes S, Zhou J, Poh MK, Sessions PF
403 de, Niyomrattanakit P, Dong H, Hoffmaster K, Goh A, Nilar S, Schul W, Jones S, Kramer L,
404 Compton T, Shi P-Y. 2011. Inhibition of Dengue Virus through Suppression of Host
405 Pyrimidine Biosynthesis. J Virol 85:6548–6556.
406 12. Karle JM, Anderson LW, Dietrick DD, Cysyk RL. 1980. Determination of serum and plasma
407 uridine levels in mice, rats, and humans by high-pressure liquid chromatography. Anal
408 Biochem 109:41–46.

409 13. Cuthbertson CR, Guo H, Kyani A, Madak JT, Arabzada Z, Neamati N. 2020. The
410 Dihydroorotate Dehydrogenase Inhibitor Brequinar Is Synergistic with ENT1/2 Inhibitors.
411 Acs Pharmacol Transl Sci 3:1242–1252.
412 14. Liu Q, Gupta A, Okesli-Armlovich A, Qiao W, Fischer CR, Smith M, Carette JE, Bassik
413 MC, Khosla C. 2020. Enhancing the Antiviral Efficacy of RNA-Dependent RNA Polymerase
414 Inhibition by Combination with Modulators of Pyrimidine Metabolism. Cell Chem Biol
415 27:668-677.e9.
416 15. Gregov D, Jenkins A, Duncan E, Siebert D, Rodgers S, Duncan B, Bochner F, Lloyd J. 1987.
417 Dipyridamole: pharmacokinetics and effects on aspects of platelet function in man. Brit J
418 Clin Pharmaco 24:425–434.
419 16. Ianevski A, Giri AK, Aittokallio T. 2020. SynergyFinder 2.0: visual analytics of multi-drug
420 combination synergies. Nucleic Acids Res 48:W488–W493.
421 17. Xiong R, Zhang L, Li S, Sun Y, Ding M, Wang Y, Zhao Y, Wu Y, Shang W, Jiang X, Shan
422 J, Shen Z, Tong Y, Xu L, Chen Y, Liu Y, Zou G, Lavillete D, Zhao Z, Wang R, Zhu L, Xiao
423 G, Lan K, Li H, Xu K. 2020. Novel and potent inhibitors targeting DHODH are broad-
424 spectrum antivirals against RNA viruses including newly-emerged coronavirus SARS-CoV-
425 2. Protein Cell 11:723–739.
426 18. Schultz DC, Johnson RM, Ayyanathan K, Miller J, Whig K, Kamalia B, Dittmar M, Weston
427 S, Hammond HL, Dillen C, Ardanuy J, Taylor L, Lee JS, Li M, Lee E, Shoffler C, Petucci C,
428 Constant S, Ferrer M, Thaiss CA, Frieman MB, Cherry S. 2022. Pyrimidine inhibitors
429 synergize with nucleoside analogues to block SARS-CoV-2. Nature 1–9.
430 19. Calistri A, Luganini A, Mognetti B, Elder E, Sibille G, Conciatori V, Vecchio CD, Sainas S,
431 Boschi D, Montserrat N, Mirazimi A, Lolli ML, Gribaudo G, Parolin C. 2021. The New

432 Generation hDHODH Inhibitor MEDS433 Hinders the In Vitro Replication of SARS-CoV-2
433 and Other Human Coronaviruses. Microorg 9:1731.
434 20. Kim Y-J, Cubitt B, Cai Y, Kuhn JH, Vitt D, Kohlhof H, Torre JC de la. 2020. Novel
435 Dihydroorotate Dehydrogenase Inhibitors with Potent Interferon-Independent Antiviral
436 Activity against Mammarenaviruses In Vitro. Viruses 12:821.
437 21. Rodriguez CO, Plunkett W, Paff MT, Du M, Nowak B, Ramakrishna P, Keating MJ, Gandhi
438 V. 2000. High-performance liquid chromatography method for the determination and
439 quantitation of arabinosylguanine triphosphate and fludarabine triphosphate in human cells. J
440 Chromatogr B Biomed Sci Appl 745:421–430.